

Article

Leaf Spot Disease of Red Clover Caused by *Leptosphaeria weimeri* (= *Longiseptatispora meliloti*) in China

Rongchun Zheng ^{1,2,3} , Zhibiao Nan ^{1,2,3} and Tingyu Duan ^{1,2,3,*}

¹ Key Laboratory of Herbage Improvement and Grassland Agroecosystems, Lanzhou University, Lanzhou 730020, China; zhengrongchun105@gmail.com (R.Z.); zhibiao@lzu.edu.cn (Z.N.)

² Key Laboratory of Grassland Livestock Industry Innovation, Ministry of Agriculture and Rural Affairs, Lanzhou 730020, China

³ College of Pastoral Agriculture Science and Technology, Lanzhou University, Lanzhou 730020, China

* Correspondence: duanty@lzu.edu.cn

Abstract: Red clover (*Trifolium pratense*) is widely cultivated as an excellent forage and green manure crop. In 2021, a leaf spot disease was discovered in a red clover field in Min County, Gansu Province, China. Symptoms on *T. pratense* manifested as small white spots that gradually expanded into nearly oval or irregularly shaped gray-white lesions. The causal agent of this new disease was identified as *Leptosphaeria weimeri* (= *Longiseptatispora meliloti*) based on morphological identification, pathogenicity tests, and the phylogenetic identification of ITS, LSU, and SSU sequence. The optimal growth temperature was found to be 20 °C under different culture conditions, while the optimal spore-producing temperature was 25 °C. The pH for optimal growth and spore production was seven. The fungus grew and produced spores successfully on both PDA and PSA media. Additionally, the pathogen was efficiently inhibited using 450 g/L of prochloraz fungicide in vitro. To our knowledge, this is the first report of leaf spot disease on red clover caused by *L. meliloti* in China.

Keywords: *Leptosphaeria weimeri* (= *Longiseptatispora meliloti*); red clover; leaf spot disease; control



Citation: Zheng, R.; Nan, Z.; Duan, T. Leaf Spot Disease of Red Clover Caused by *Leptosphaeria weimeri* (= *Longiseptatispora meliloti*) in China. *Agronomy* **2024**, *14*, 1055. <https://doi.org/10.3390/agronomy14051055>

Academic Editor: Robert P. Larkin

Received: 16 April 2024

Revised: 8 May 2024

Accepted: 13 May 2024

Published: 16 May 2024



Copyright: © 2024 by the authors. Licensee MDPI, Basel, Switzerland. This article is an open access article distributed under the terms and conditions of the Creative Commons Attribution (CC BY) license (<https://creativecommons.org/licenses/by/4.0/>).

1. Introduction

Red clover (*Trifolium pratense*) is a perennial herb belonging to the Leguminosae family. It stands as one of the most important cultivated legume forages in Europe, the United States, Canada, Australia, and New Zealand [1]. China also extensively cultivates red clover. However, fungal diseases substantially constrain its growth and yield, thereby impacting its overall productivity and quality. By 2022, global reports from Fungal Databases (<https://nt.ars-grin.gov/fungaldatabases/>, accessed on 1 December 2022) have documented over 100 fungal pathogens causing more than 50 diseases in red clover. Notable among these are powdery mildew caused by *Erysiphe* spp., root rot caused by *Fusarium* spp., southern blight caused by *Colletotrichum* spp., and *Sclerotinia* rot caused by *Sclerotinia* spp., contributing to significant losses in red clover production in Europe, the United States, India, and other regions [2–5].

Leptosphaeriaceae, an economically significant family of plant pathogens within the order Pleosporales, poses a substantial threat. Some species within this family also act as endophytes or saprobes on various host plants [6]. The genus *Leptosphaeria*, belonging to the Leptosphaeriaceae family, infects various parts of legume crops, including the leaves, stems, root crowns, and roots, leading to conditions like leaf spot, crown rot, and root rot [7,8]. Notable species like *L. maculans* and *L. biglobosa* cause blackleg and stem canker, severely impacting oilseed Brassicas, particularly canola (*B. napus* and *B. rapa*) [9]. Moreover, the mitotic sporulating fungus *Phoma macdonaldii* (Teleomorph: *L. lindquistii*) poses a threat to sunflower (*Helianthus annuus*) and has been associated with premature plant death and yield losses [10,11]. Recent reports by Claassen [12] have identified a new disease of *Rorippa curvisiliqua* caused by *Leptosphaeria* spp.

Taxonomy within the Leptosphaeriaceae family remains challenging due to a limited understanding of crucial morphological characters for taxonomic differentiation and a lack of reference strains. Sequences of the entire ITS region, including the 5.8S rDNA of *Leptosphaeria* isolates and other closely related *Leptosphaeria* and *Phaeosphaeria* species, were used to construct a phylogenetic tree using parsimony and distance analyses to determine the phylogenetic relationships [13,14]. While the ITS locus, especially for the nuclear ribosomal RNA gene sequences (ITS, LSU, and SSU), served as a universal DNA barcode for fungi [15] and is the most widely sequenced marker for fungi, it may not suffice for distinguishing closely related species within *Leptosphaeria*, also known as phoma-like fungi, necessitating the identification of alternative DNA loci [16,17]. Therefore, identifying an alternative DNA locus (or secondary DNA marker) has been a promising approach [18]. Phylogenetic analyses using additional markers like the *RPB2*, *EF-1 α* , *ACT*, and β -tubulin regions have been employed to establish evolutionary relationships and provide a backbone tree for *Leptosphaeria* and allied genera [6,19,20].

Chemical control plays a pivotal role in integrated disease management due to its rapid action, simplicity, and lack of regional and seasonal restrictions. Methods like carbendazim seed treatment have proven effective against crown rot and powdery mildew and can enhance red clover seed yield when combined with foliar sprays of wettable sulfur or hexaconazole [5]. Additionally, seed treatment before sowing effectively controls seed-borne pathogens, thereby enhancing seedling emergence [21]. Greenhouse experiments have demonstrated the efficacy of fungicides like Panocrine 400 and Rovral Flo in inhibiting seedling root infestations by *Fusarium*, *Phoma*, and *Alternaria*, resulting in the decreased severity of root diseases [22]. Chemical fungicides can effectively control diseases to a certain extent, but improper application can lead to pathogen resistance. In contrast, antibiotics and biological control agents are gaining attention, owing to their potential to enhance agricultural sustainability.

Our study aimed to identify the pathogen causing leaf spot on red clover through morphological and molecular characterization, with additional objectives including assessing the efficacy of eight fungicides and antibiotics against the pathogen in vitro and the exploration of the biological characteristics of the pathogen.

2. Materials and Methods

2.1. Field Survey, Diseased Leaf Collection, and Pathogen Isolation

Leaf spot disease was discovered in red clover fields planted in Min County, Gansu Province, in May 2021. Five plots (1 m \times 1 m) were randomly chosen to examine disease incidence using a 5-point sampling method. Within each plot, 50 leaves of red clover were randomly chosen for each point to assess both the incidence and severity of the disease. Subsequently, the incidence rate (I) and disease index (DI) were computed utilizing the following formulas [23]:

$$I (\%) = (\text{number of diseased leaves} / \text{total number of leaves investigated}) \times 100 \quad (1)$$

$$DI = [\text{sum (class frequency} \times \text{score of rating class)}] / [(\text{total number of leaves investigated}) \times 5] \times 100 \quad (2)$$

The following disease scale of 0 to 5 class was used: 0 = healthy, 1 = 0 to 20% of leaf area affected, 2 = 21 to 40%, 3 = 41 to 60%, 4 = 61 to 80%, and 5 = 81 to 100%.

Diseased leaves were promptly collected, and the infected tissue was prepared by cutting it into 3 \times 3 mm pieces. Subsequently, these pieces underwent surface sterilization using 75% ethanol for 30 s, followed by 5% commercial bleach (NaOCl) for 2 min. After thorough rinsing with sterilized distilled water, the samples were dried with sterilized filter paper. The diseased tissue was then cultured on potato dextrose agar (PDA) and incubated at 25 °C in darkness for 10 days, leading to the isolation of a fungus from the diseased leaves, with isolation frequencies ranging from 80% to 100%. A total of eight isolates were acquired, with MXK7 chosen for subsequent experiments owing to its optimal growth conditions.

2.2. Morphological and Molecular Characterization

The identification of the isolates at the species level was achieved through an examination of the morphology, supplemented by molecular phylogenetic analysis. Colony traits were meticulously assessed by observing cultures on PDA plates after 20 days of incubation at 25 °C in darkness. A small amount of mycelium was collected using a pin and positioned on a slide with a drop of sterile water to prepare for microscopic observation. The observation and recording of the hyphae and conidia were conducted using Olympus XZ251 (40×, Olympus Corporation, Tokyo, Japan) with a digital camera. Furthermore, three strains containing MXK7 (MXK5, MXK6, and MXK7) underwent targeted DNA sequence amplification and sequencing.

Mycelia from fresh colonies were carefully collected from the PDA medium using sterile slides for subsequent DNA extraction. Genomic DNA extraction for fresh samples was performed using a Fungal DNA Kit (Sangon Biotech Shanghai, Shanghai, China) following the manufacturer's instructions. DNA concentration, ranging from 50 to 200 ng/μL, was measured using a NanoDrop 2000 spectrophotometer (Thermo Scientific, Waltham, MA, USA). DNA sequences from the internal transcribe spacer (ITS), small subunit (SSU), and large subunit (LSU) of the nuclear ribosomal RNA genes were obtained, utilizing specific primer sets for each region (Table 1). The ITS region was amplified using ITS4/ITS5 primers [24], the SSU region was amplified using NS1/NS4 primers [25,26], and the LSU region was amplified using LR0R/LR5 primers [27]. PCR amplifications were carried out using a T100 thermal cycler (Bio-Rad, Hercules, CA, USA) (1 μL DNA, 1 μL each of forward and reverse primers, 12.5 μL PCR MasterMix, and 9.5 μL ddH₂O), and PCR products were subjected to visualization through electrophoresis on a 1% agarose gel, purification, and bidirectional sequencing by Sangon Biotech Shanghai, China. The gene sequences were assembled and manually adjusted using Seqman (DNASTAR 11.0, Seqman Pro) and MEGA v.11, respectively. Maximum likelihood phylogenies were inferred using IQ-TREE [28] under the Edge-linked partition model for 1000 ultrafast bootstraps [29]. Bayesian inference phylogenies were inferred using MrBayes 3.2.6 [30] under the partition model, with 2 parallel runs and 100,000 generations, discarding the initial 25% of sampled data as burn-in [31]. The resulting phylogenetic tree was edited and annotated in figtree v1.4.4 and Adobe Illustrator 2023.

Table 1. List of primers used in this study.

Gene	Primer	Sequence (5'-3')	References
<i>nrSSU</i>	NS1	GTAGTCATATGCTTGTCCTC	[25,26]
	NS4	CTCCGTC AATTCCTTTAAG	
<i>nrLSU</i>	LR0R	GTACCCGCTGAACTTAAGC	[27]
	LR5	ATCCTGAGGGAAACTTC	
ITS	ITS4	TCCTCCGCTTATTGATATGC	[24]
	ITS5	GGAAGTAAAAGTCGTAACAAGG	

2.3. Biological Characteristics

The effect of different culture media, temperatures, pH, carbon sources, and nitrogen sources on the biological characteristics of strain MXK7 were assessed individually. Isolated colonies were purified by selecting the fresh 4 mm mycelial cakes using a sterilized borer from the colony edge and reculturing them on various media, including PDA, plate count agar (PCA), corn meal agar (CMA), oatmeal agar (OMA), Czapek–Dox agar (CZA), and malt extract agar (MEA).

Czapek–Dox medium with the carbon or nitrogen source replaced served as the control. Carbon sources tested included sucrose, D-glucose, D-fructose, D-galactose, D-maltose, D-lactose, D-sorbitol, and soluble starch, while nitrogen sources comprised potassium nitrate, ammonium sulfate, ammonium chloride, diammonium hydrogen phosphate, peptone, urea, glycine, and sodium nitrate. Hyphae were transferred onto a PDA plate and incubated at temperatures ranging from 5 °C to 35 °C for 20 days. The pH of the sterilized PDA

medium was adjusted to 4, 6, 7, 8, 10, 11, and 12 using 1 mol/L HCl and 1 mol/L NaOH solutions under aseptic conditions.

Each treatment was replicated four times, and all treatments were incubated at a constant temperature of 25 °C in the dark for 20 days. The initial measurement was taken on the third day of culturing, followed by three more measurements every two days. Colony diameter measurement and growth rate calculation were performed following the method described by Xue [32]. All data were compared using the Duncan test ($p < 0.05$) and analyzed with SPSS Statistics 28.

2.4. Greenhouse Pathogenicity Tests

The test variety utilized was *Trifolium pretense* (CV. Minshan), harvested from the fields of Min County in autumn 2020. Seeds were chosen for their robustness and integrity, undergoing a series of treatments, as follows: soaking in 75% alcohol for 30 s, disinfection with 10% hydrogen peroxide (H₂O₂) solution for 10 min, and rinsing with sterilized water five times. Subsequently, the seeds were placed in petri dishes lined with two layers of sterilized filter paper, moistened with sterile water, and then incubated in a plant incubator maintained at 25 °C and 65% humidity for two days. Humidity levels were upheld by daily water additions. Upon germination, the seeds were sown with eight seeds per pot, and three plants were planted after seedling emergence.

For the pathogenicity test, strain MXK7 was cultured on PDA medium at 25 °C for 20 days. Conidia were collected by adding 10 mL of sterile water to a culture plate, scraping with a sterile glass slide to release conidia, followed by dilution and counting using a hemocytometer. The spore suspension was adjusted to 1×10^6 spores/mL, and the count was repeated thrice. Next, 20 mL of 1×10^6 spores/mL was evenly sprayed onto healthy red clover leaves, with 0.02% Tween 80 solution added to enhance adhesion. Sterilized water with 0.02% Tween 80 solution served as the blank control. Disease progression on the leaves was monitored, and the incidence rate was calculated regularly every two days starting at 48 h after inoculation.

2.5. Sensitivity Testing of Fungicides

Eight fungicides and antibiotics were prepared separately in sterilized water, mixed evenly, and diluted fivefold. The plates were prepared as follows: under aseptic conditions, 99 mL of sterilized PDA medium at 50 to 60 °C was put into a blue cap bottle, and then 1 mL of each solution of each fungicide was added in and mixed thoroughly, after which, approximately 20 mL was poured into each 90-mm sterile culture dish. Pathogen colonies (4 mm in diameter) were placed at the center of the PDA medium containing fungicides and cultured for 20 days at 25 °C and 75% relative humidity in darkness. The mycelial growth inhibition rate (MGIR, %) was calculated following the method described by Zhang et al. [33]; the formula is as follows:

$$\text{MGIR (\%)} = (\text{control colony diameter} - \text{treated colony diameter}) / \text{control colony diameter} \times 100 \quad (3)$$

The probability of MGIR was set as Y , and the concentration of each fungicide was set as X to establish the regression equation using the regression method and calculate the EC₅₀ values [34]. All data in this study were analyzed using IBM SPSS Statistics v.20.

3. Results

3.1. Disease Survey

In May 2021, leaf spot disease was detected in the red clover fields planted in Min County, Gansu Province, with an initial incidence rate of 0.80% (Figure 1). The disease predominantly affects the leaves, manifesting initially as small white spots that gradually expand to form near-oval or irregularly shaped gray-white lesions bordered by a faint black margin (Figure 2a,b). The central area of these lesions appears lighter in color (Figure 2c). The incidence rate peaked in August at 4.20%, and the disease index ranged

from 0.23 to 1.23. In 2022, the incidence rate progressively increased from 1.30% in May to a peak of 4.80% in August, with the disease index escalating from 0.50 to 1.53 (Figure 1). In the advanced stages, red clover leaves desiccated and cracked. Overall, this leaf spot disease exhibited an upward trend in progression, although both the incidence rate and the disease index remained extremely low.

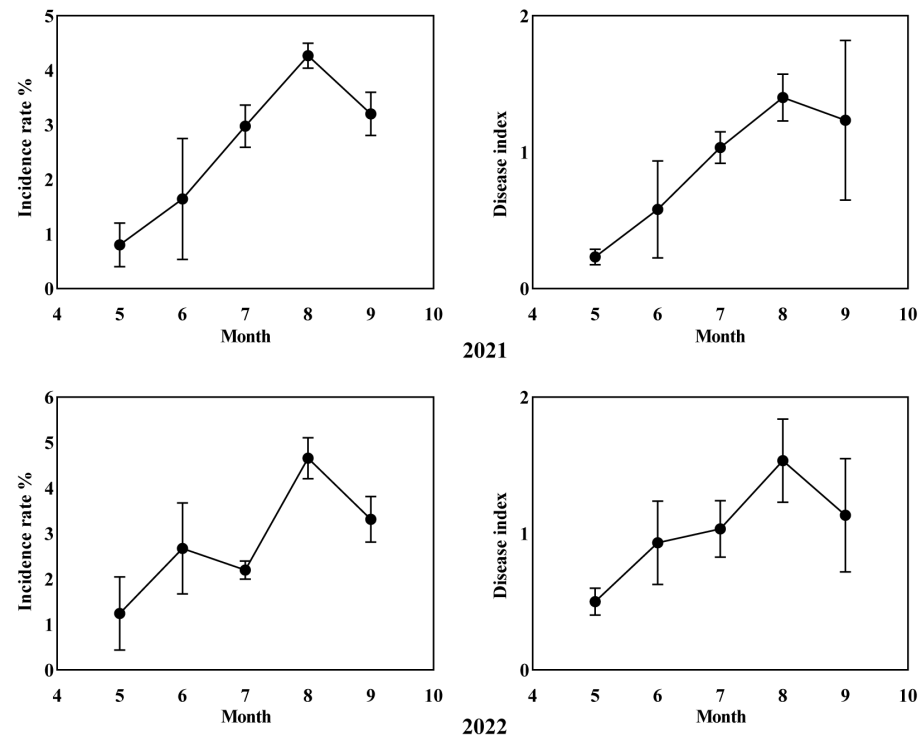


Figure 1. Incidence and disease index of red clover leaf spot disease in the fields in the years 2021 and 2022.



Figure 2. Symptoms of red clover leaf spot disease. (a,b) Symptoms in the fields; (c) symptoms under microscopy.

3.2. Isolation and Identification of the Pathogen

A fungus was isolated from the diseased leaves at a frequency of 80% to 100%. On PDA medium, the pathogen's mycelium appears felt-like, exhibiting slow growth resulting in relatively small colony areas, ranging in color from pink to off-white (Figure 3a,b). The colony surface is wrinkled and thick, and the mass of spores was produced and released from luminal or stalk-like sites (Figure 3c,d). The spores were approximately $6\text{--}15 \times 1\text{--}3 \mu\text{m}$ in size, colorless, with one or no septa, and elliptical to ovoid (Figure 3e–k).

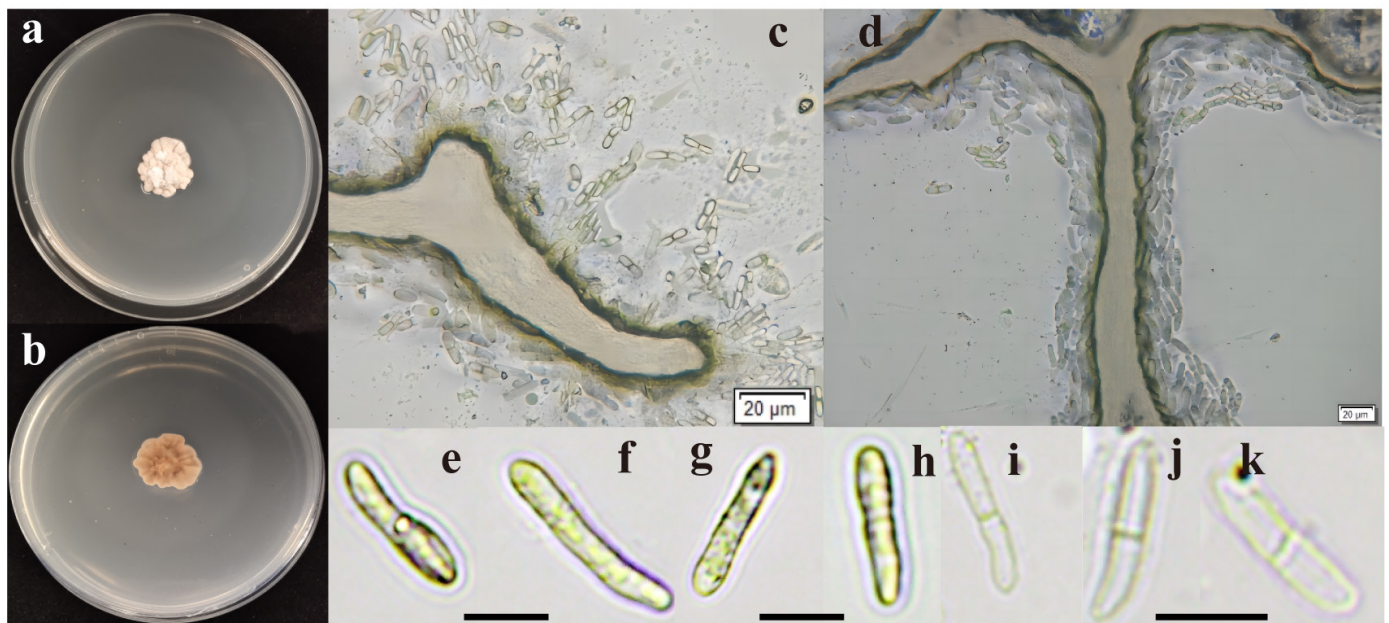


Figure 3. Morphological characteristics of *L. meliloti*. (a,b) Front and back of a colony of *L. meliloti* cultivated on PDA for 20 days in the dark at 25 °C; (c,d) spores are produced and released from luminal or stalk-like sites; (e–k) conidia (the black scale in the figures represent 5 µm).

A sequence alignment analysis of strains was conducted based on ITS, LSU, and SSU genes. The reference strains were obtained from GenBank and previous research (Table 2) for constructing the ITS–SSU–LSU phylogenetic tree [6,15]. The results indicated that strains MXK5, MXK6, and MXK7, along with *L. meliloti* sampled from various locations, clustered into a single group with a self-sustaining rate of 100% BS and 100%/1 BI (Figure 4), supporting the morphological and molecular identification.

Table 2. Reference isolates used in this study and their GenBank accession numbers.

Taxon	Culture Strains	LSU	ITS	SSU
<i>Didymella exigua</i>	GU237794.1	EU754155.1	GU237794.1	EU754056.1
<i>Leptosphaeria conoidea</i>	JF740201.1	JF740279.1	JF740201.1	JF740099.1
<i>Leptosphaeria doliolum</i>	KT454727.1	KT454719.1	KT454727.1	KT454734.1
<i>Leptosphaeria doliolum</i>	JF740205.1	GQ387576.1	JF740205.1	GU296159.1
<i>Leptosphaeria ebuli</i>	NR_155323.1	KP744488.1	NR_155323.1	KP753954.1
<i>Leptosphaeria regiae</i>	MN244201.1	MN244171.1	MN244201.1	MN244177.1
<i>Leptosphaeria slovacica</i>	JF740247.1	JF740315.1	JF740247.1	JF740101.1
<i>Leptosphaeria sydowii</i>	MT185517.1	MT183480.1	MT185517.1	MT214959.1
<i>Leptosphaeria urticae</i>	OQ401052.1	OQ411135.1	OQ401052.1	OQ411131.1
<i>Leptosphaeria urticae</i>	MK123333.1	MK123332.1	MK123333.1	MK123329.1
<i>Longiseptatispora meliloti</i>	MT223814.1	MT223909.1	MT223814.1	-
<i>Neophaeosphaeria filamentosa</i>	JF740259.1	GQ387577.1	JF740259.1	GQ387516.1
<i>Paraleptosphaeria rubi</i>	KT454726.1	KT454718.1	KT454726.1	KT454733.1
<i>Phoma herbarum</i>	FJ427022.1	KF251715.1	FJ427022.1	EU754087.1
<i>Plenodomus chrysanthemi</i>	NR_111622.1	GU238151.1	NR_111622.1	GU238230.1
<i>Plenodomus guttulatus</i>	KT454721.1	KT454713.1	KT454721.1	KT454729.1
<i>Plenodomus salviae</i>	KT454725.1	KT454717.1	KT454725.1	KT454732.1
<i>Plenodomus visci</i>	NR_119957.1	EU754195.1	NR_119957.1	EU754096.1

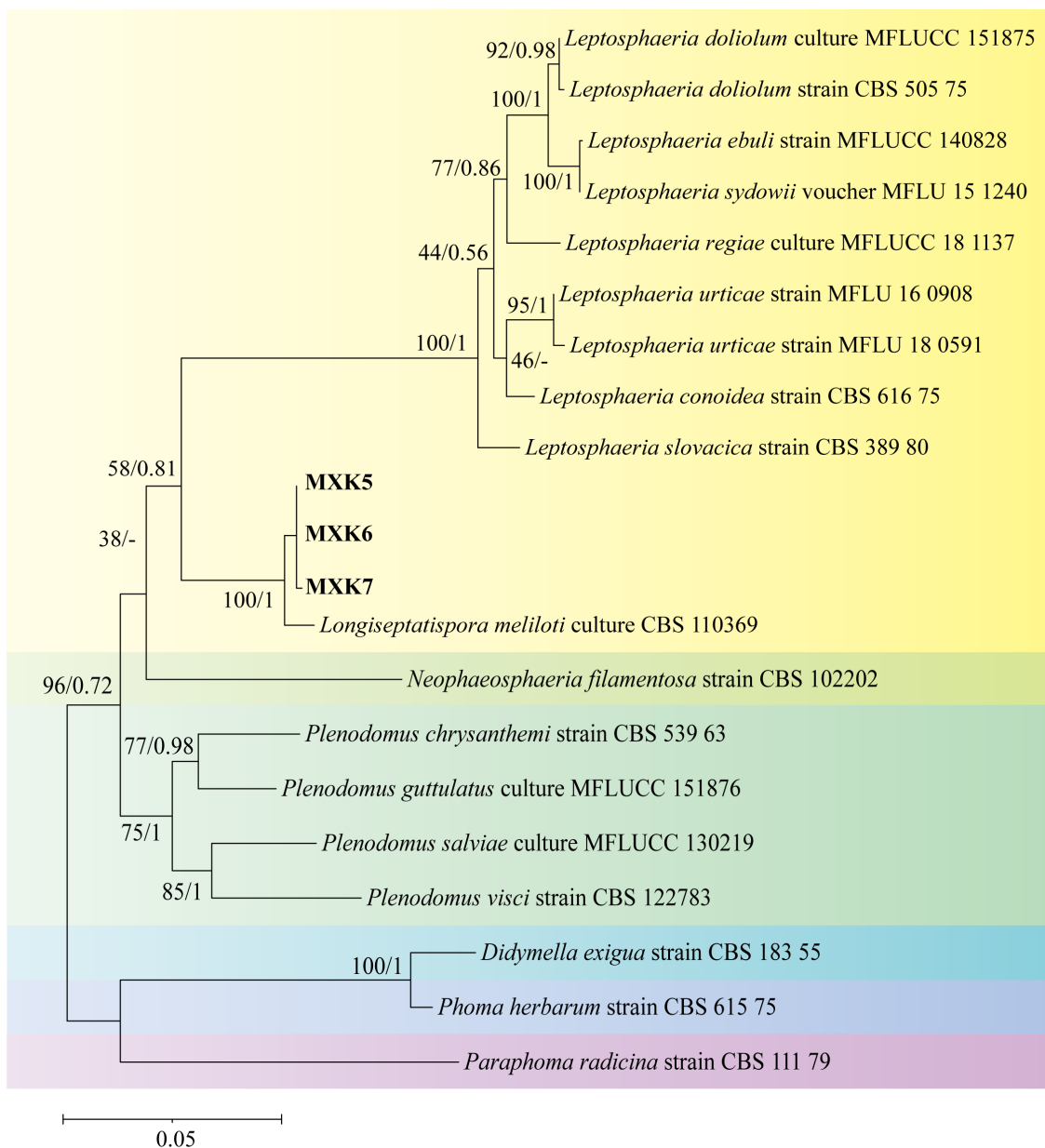


Figure 4. Maximum-likelihood (ML) phylogenetic tree of the *Leptosphaeria* or *Longiseptatispora* species based on the combined sequence of LSU, SSU, and ITS. The node shows bootstrap support (BS) values and Bayesian inference (BI) scores. Different colors in the figure represent different genus of fungi.

3.3. Biological Characteristics

For the tested temperature, pH, and growth media, the optimum growth temperature for *L. meliloti* is 20 °C, while the most favorable temperature for sporulation is 25 °C. The ideal pH for both growth and sporulation is seven. The best medium for spore production is PDA, while PSA is the optimal medium for mycelial growth (Table 3, Figure 5). The pathogen efficiently utilizes carbon sources such as maltose, fructose, galactose, and soluble starch, as well as nitrogen sources such as peptone, glycine, and sodium nitrate (Figure 5). It does not produce spores in any of the tested Czapek–Dox medium with the carbon and nitrogen source conditions replaced (Table 3).

Table 3. Fungicide concentration gradient used for test.

Growth Condition		Growth Rate (mm/20 d)	Spore Production ($\times 10^5/\text{mL}$)
Culture media	PDA	9.13 \pm 0.64 c	7.94 a
	PSA	11.28 \pm 0.94 a	-
	WA	8.05 \pm 0.81 d	-
	Czapek	8.14 \pm 0.40 d	-
	CMA	7.9 \pm 0.57 d	3.88 b
	OMA	9.67 \pm 0.30 b	0.56 c
pH values	10	26.34 \pm 1.86 c	-
	8	32.19 \pm 1.17 b	0.08 c
	7	38.55 \pm 1.03 a	6.70 a
	6	8.79 \pm 0.73 e	2.69 b
	4	14.53 \pm 0.89 d	-
Temperatures ($^{\circ}\text{C}$)	5	3.00 \pm 0.00 e	-
	10	6.65 \pm 0.50 d	-
	15	7.95 \pm 0.61 c	4.56 b
	20	13.71 \pm 0.33 a	4.44 b
	25	8.81 \pm 0.74 b	7.94 a
	30	3.00 \pm 0.00 e	-
Carbon source	Sucrose	8.14 \pm 0.40 c	-
	Glucose	9.50 \pm 0.64 a	-
	Sorbitol	8.24 \pm 1.01 bc	-
	Fructose	8.60 \pm 0.43 bc	-
	Lactose	8.37 \pm 0.40 bc	-
	Galactose	6.20 \pm 0.48 d	-
	Soluble starch	8.35 \pm 0.35 bc	-
	Maltose	8.85 \pm 0.47 b	-
Nitrogen source	KNO ₃	8.14 \pm 0.40 c	-
	Peptone	9.97 \pm 0.57 a	-
	NH ₄ Cl	6.87 \pm 0.47 d	-
	NH ₄ H ₂ PO ₄	7.88 \pm 0.57 c	-
	Urea	3.00 \pm 0.00 f	-
	(NH ₄) ₂ SO ₄	5.71 \pm 0.36 e	-
	Glycine	9.67 \pm 0.50 a	-
	NaNO ₃	9.17 \pm 0.40 b	-

Notes, Different lowercase letters indicate significant differences between different treatments ($p < 0.05$).

3.4. Pathogenicity Testing

Ten days after inoculation, the leaves inoculated with the spore suspension exhibited symptoms with an incidence rate of 2% and no longer developing. The lesions manifested as irregularly shaped grayish-brown spots on the margins of the leaves (Figure 6b), somewhat similar to those previously recorded in Min Country, while no symptoms were found in the control plants (Figure 6a). However, the same pathogen was re-isolated from the lesions and confirmed by both morphology and molecular identification as *L. meliloti*, thus fulfilling Koch's postulates.

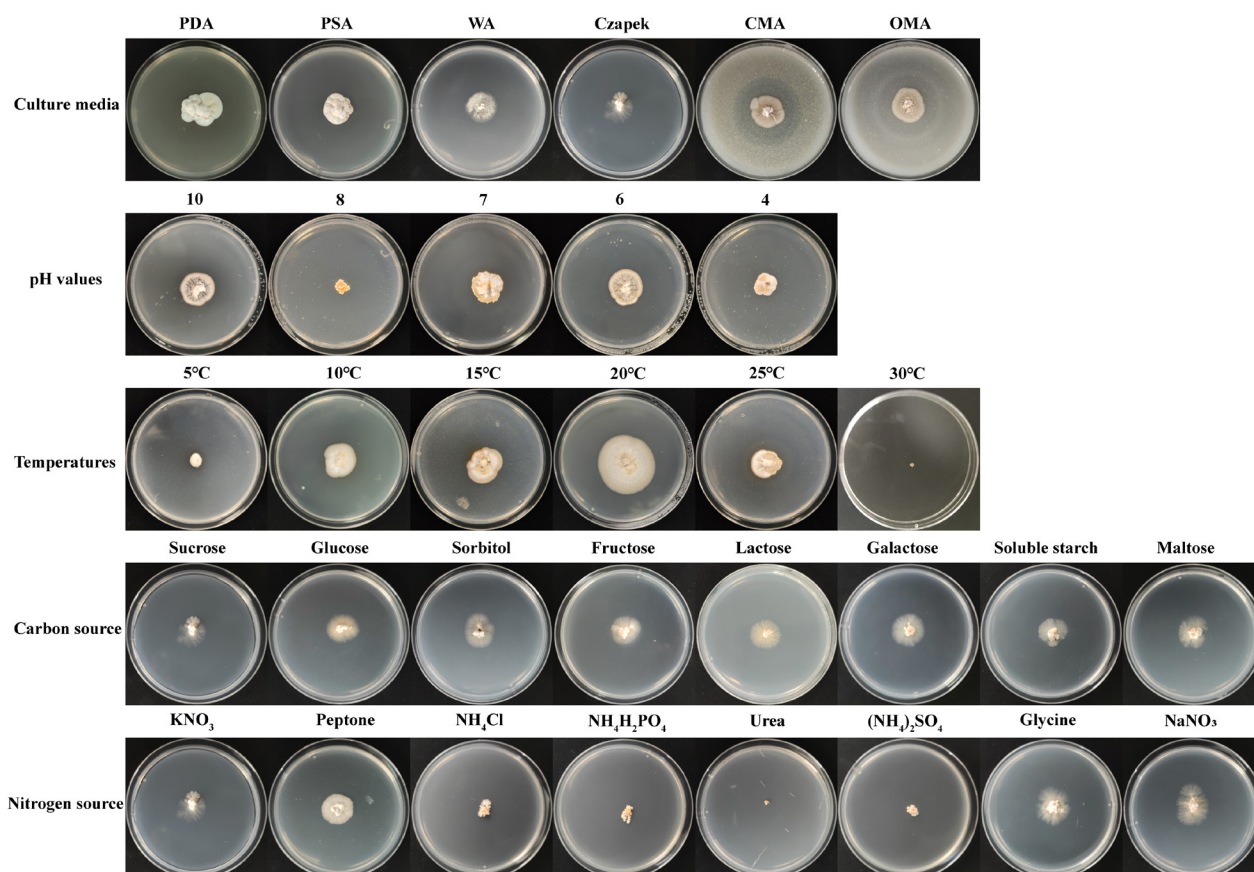


Figure 5. Growth of colonies cultured on different media, pH values, and temperatures, carbon sources, and nitrogen sources (front side).



Figure 6. Symptoms on red clover after inoculating with isolates of MXK7 in a greenhouse. (a) Inoculated with sterilized water; (b) inoculated with spore suspension (red circle).

3.5. Effects of Eight Fungicides and Antibiotics on Mycelia Growth

Compared with the control treatment, eight fungicides and antibiotics differentially inhibited mycelial growth, with MGIR ranging from 0.72 to 62.89%, and the inhibitory effect increased with concentration (Table 4). A total of 450 g/L prochloraz exhibited significant antifungal activity with an EC₅₀ value of 0.6424 mg/L, followed by 10% difenoconazole with an EC₅₀ value of 0.8821 mg/L, while 6% kasugamycin was the least, with an EC₅₀ of 328.0198 mg/L. Based on the regression equations, the slope of the 450 g/L prochloraz was the steepest at 0.2133, while the slope of the 250 g/L azoxystrobin was the smallest

at 0.1012, indicating that *L. meliloti* was most sensitive to prochloraz and least sensitive to azoxystrobin (Table 5).

Table 4. Fungicide and antibiotic concentration gradients used for test.

Fungicides	Concentration (mg/L)	Colony Diameters (mm)	Inhibition Rate (%)
CK	0	18.18	-
450 g/L Prochloraz	0.0064	17.68 ± 0.40 a	2.75 ± 2.25 e
	0.032	14.63 ± 0.55 b	19.53 ± 3.15 d
	0.16	9.29 ± 0.88 c	48.91 ± 4.98 c
	0.8	8.24 ± 0.23 d	54.69 ± 1.03 b
	4	7.32 ± 0.31 e	59.73 ± 1.86 a
10% Difenoconazole	0.0064	17.17 ± 0.39 a	5.59 ± 2.55 e
	0.032	13.98 ± 0.27 b	23.10 ± 1.41 d
	0.16	11.72 ± 0.53 c	35.53 ± 3.14 c
	0.8	8.23 ± 0.35 d	54.74 ± 1.94 b
	4	7.58 ± 0.25 e	58.33 ± 1.47 a
50% Carbendazim	0.032	17.04 ± 0.17 a	6.28 ± 0.08 e
	0.16	15.05 ± 0.89 b	17.22 ± 0.50 d
	0.8	12.86 ± 0.14 c	29.29 ± 0.80 c
	4	10.60 ± 0.36 d	41.69 ± 2.13 b
	20	6.88 ± 0.21 e	62.18 ± 1.17 a
70% Thiophanate-methyl	0.16	18.05 ± 0.16 a	0.72 ± 0.01 e
	0.8	16.55 ± 0.42 b	8.99 ± 2.40 d
	4	15.56 ± 0.54 c	14.45 ± 2.81 c
	20	11.57 ± 0.71 d	36.37 ± 4.10 b
	100	7.08 ± 0.28 e	61.08 ± 1.47 a
250 g/L Azoxystrobin	0.16	12.44 ± 0.40 a	31.57 ± 2.01 e
	0.8	10.44 ± 0.40 b	42.57 ± 2.01 d
	4	9.71 ± 0.22 c	46.61 ± 1.03 c
	20	8.63 ± 0.43 d	52.53 ± 2.34 b
	100	6.92 ± 0.34 e	61.94 ± 2.23 a
6% Kasugamycin	0.08	15.58 ± 0.48 a	14.32 ± 2.71 e
	0.4	14.72 ± 0.30 b	19.04 ± 1.41 d
	2	13.63 ± 0.25 c	25.02 ± 1.41 c
	10	12.21 ± 0.36 d	32.83 ± 2.14 b
	50	10.23 ± 0.47 e	43.74 ± 2.73 a
80% Ethylclicin	0.08	17.03 ± 0.21 a	6.33 ± 1.03 e
	0.4	15.61 ± 0.51 b	14.15 ± 2.73 d
	2	13.35 ± 0.41 c	26.56 ± 2.43 c
	10	11.19 ± 0.57 d	38.48 ± 3.01 b
	50	8.18 ± 0.28 e	55.04 ± 1.79 a
0.3% Tetramycin	0.08	16.76 ± 0.62 a	7.84 ± 3.40 d
	0.4	14.73 ± 0.32 ab	18.98 ± 1.60 cd
	2	13.14 ± 0.38 bc	27.72 ± 2.16 bc
	10	11.89 ± 3.81 c	34.63 ± 20.99 b
	50	6.75 ± 0.29 d	62.89 ± 1.67 a

Notes, Different lowercase letters indicate significant differences between different concentrations of the fungicide ($p < 0.05$).

Table 5. Toxicity of different fungicides and antibiotics on strain MXK7.

Fungicides	Regression Equation	r	EC ₅₀ (mg/L)	95% Confidence Intervals
450 g/L Prochloraz	$y = 0.2133x + 0.5410$	0.9527	0.6424	0.4421–0.9970
10% Difenoconazole	$y = 0.1962x + 0.5107$	0.9845	0.8821	0.7781–0.9990
50% Carbendazim	$y = 0.1949x + 0.3322$	0.9913	7.2611	0.8690–0.9995
70% Thiophanate-methyl	$y = 0.2119x + 0.1157$	0.9588	65.1029	0.4965–0.9974
250 g/L Azoxystrobin	$y = 0.1012x + 0.4096$	0.9884	7.8217	0.8298–0.9993
6% Kasugamycin	$y = 0.1039x + 0.2386$	0.9863	328.0198	0.8008–0.9991
80% Ethylclicin	$y = 0.1742x + 0.2287$	0.9926	36.0911	0.8883–0.9995
0.3% Tetramycin	$y = 0.1799x + 0.2500$	0.9588	24.5301	0.4970–0.9974

4. Discussion

In this study, the pathogen of red clover leaf spot disease was identified as *L. weimeri* (= *L. meliloti*) through morphological comparison, molecular identification, and a pathogenicity test. This marks the first documented instance of red clover leaf spot caused by *L. meliloti* in China.

According to the Index Fungorum (www.indexfungorum.org, accessed on 31 January 2024), *L. weimeri* stands as a legitimate and distinct species without any synonyms or anamorphs. This stands in contrast to the findings of Schoemaker et al. [35], who delineated a new species, *Massarina walkeri* (= *Acrocalymma walkeri*), discovered in *Medicago sativa*. It is distinct from *L. pratensis* and the newly recognized *L. weimeri*, as well as *L. viridella* (= *P. viridella*, 1984). These assertions diverge from the conclusions drawn by Boerema [36], who synonymized *L. weimeri* and *Stagonospora meliloti* (1920). Subsequently, there has been a steady stream of research confirming the anamorph–teleomorph connection between *L. weimeri* and *P. meliloti* (= *L. meliloti*, 2020) [20,37,38].

Currently, *L. meliloti* is solely reported on Leguminosae plants such as *Medicago*, *Trifolium*, *Lupinus*, and *Melilotus* (based on the Fungaldatabase). Shang [39] reported a novel disease of white clover (*Trifolium repens*) caused by *S. meliloti* and dubbed Stagonospora leaf spot, in China. Its teleomorph was identified as *L. weimeri*, although it was not cultured from the infected leaves. The disease has been reported widely in the United States and Europe, affecting various leguminous forage crops. The pathogen has caused morbidity and yield loss in alfalfa in Australia and France [40,41] and has inflicted severe damage on white clover in Alabama, USA [42]. Apart from leaf damage, the pathogen also infects stems, root crowns, and roots, causing foot rot and root rot, which, in severe cases, result in plant death and stunting. Furthermore, the pathogen can be transmitted via seed, necessitating seed testing upon introduction [43,44]. Research on *L. meliloti* in red clover has been largely confined to disease records, with limited in-depth investigations and scant reports. To date, there are no records of this disease afflicting red clover in China. In the red clover fields of Min County, the overall incidence and severity of Longiseptatispora leaf spot were low, albeit noticeable symptoms were observed throughout the growing season, exerting minimal impact on red clover production. In greenhouse pathogenicity tests, symptoms emerged on red clover seven days after inoculation with *L. meliloti*; however, the disease did not exacerbate as the plants matured, indicating relatively low severity of the disease.

Temperature plays a pivotal role in disease dissemination. Under natural conditions, it influences infection, colonization, lesion expansion, and pathogen spread [45,46]. Results revealed that the optimum growth temperature and the optimum spore production temperature were 20 °C and 25 °C respectively. *L. meliloti* strains exhibit a narrow temperature adaptation range, thriving in the alpine and cool climates of Min County. Studies on its biological characteristics aid in understanding the environmental and nutritional conditions conducive to pathogen survival and spore production, thereby facilitating disease management. The pathogen displayed poor growth under varied nitrogen and carbon source conditions, characterized by sparse mycelium and small colonies. Its optimal pH was seven, and the preferred media included PSA and PDA. Incorporating colony morphology will streamline subsequent morphological identification of the fungus.

Of the eight selected fungicides and antibiotics, synthetic fungicides demonstrate high efficiency. They antagonize pathogenic fungi by disrupting mycelium formation, impeding cell division, inhibiting mitochondrial respiration, and suppressing ergosterol or sterol biosynthesis [47–49]. In the virulence test against *L. meliloti*, miconazole and metronidazole phenyl ether were highly effective, while chunramycin proved the least effective. Tetramycin, ethylcin, and metribuzin demonstrated poor performance. These findings suggest that *L. meliloti* is sensitive to methoxyacrylates and imidazoles but insensitive to antibiotics and benzimidazoles. It is important to note that the most efficacious fungicide was also the most soluble in water in this experiment. The solubility of fungicides in water is limited, and there are instances in which the concentration gradients of the suspensions used for experimental purposes surpass the solubility [50,51]. Consequently,

when conducting fungicide sensitivity experiments using water as a solvent, it is crucial to consider the potential impact of solubility on the results or dissolve fungicides in DMSO or an organic solvent like acetone. The results mentioned above were obtained from indoor testing; the utilization of the fungicides in the field requires consideration of factors such as local climate, product cost, and application methods, which are critical for disease control and prevention.

5. Conclusions

To the best of our knowledge, this is the first report of *L. meliloti* causing leaf spot disease on red clover in China. The field incidence of the disease was 4.80%, with the prevalence and resultant damage deemed not severe. Prochloraz and difenoconazole fungicides emerge as viable options for red clover leaf spot disease management. This study furnishes valuable insights into pathogen identification, pathogenicity, and disease occurrence.

Author Contributions: R.Z. performed the experiment and data analyses. R.Z., Z.N. and T.D. wrote and edited the manuscript. All authors have read and agreed to the published version of the manuscript.

Funding: Funding for this research was provided by the China Modern Agriculture Research System (CARS-22 Green Manure).

Data Availability Statement: All applicable data are published and referenced in the paper.

Conflicts of Interest: The authors declare no conflicts of interest.

References

- McKenna, P.; Cannon, N.; Conway, J.; Dooley, J. The use of red clover (*Trifolium pratense*) in soil fertility-building: A Review. *Field Crop. Res.* **2018**, *221*, 38–49. [\[CrossRef\]](#)
- Coulman, B.E.; Lambert, M. Selection for resistance to root rot caused by *Fusarium* spp. in red clover (*Trifolium pratense* L.). *Can. J. Plant Sci.* **1995**, *75*, 141–146. [\[CrossRef\]](#)
- Jacob, I.; Hartmann, S.; Struck, C. Response of different fodder legume species to *Colletotrichum trifolii*. *Crop. Pasture Sci.* **2016**, *67*, 1110–1115. [\[CrossRef\]](#)
- Hartmann, S.; Schubiger, F.X.; Grieder, C.; Wosnitza, A. A decade of variety testing for resistance of red clover to southern anthracnose (*Colletotrichum trifolii*) at the Bavarian state research center for agriculture. *Agriculture* **2022**, *12*, 249. [\[CrossRef\]](#)
- Bhardwaj, N.R.; Banyal, D.K.; Roy, A.K. Integrated management of crown rot and powdery mildew diseases affecting red clover (*Trifolium pratense* L.). *Crop. Prot.* **2022**, *156*, 105943. [\[CrossRef\]](#)
- Ariyawansa, H.A.; Phukhamsakda, C.; Thambugala, K.M.; Bulgakov, T.S.; Wanasinghe, D.N.; Perera, R.H.; Mapook, A.; Camporesi, E.; Kang, C.J.; Jones, E.B. Revision and phylogeny of Leptosphaeriaceae. *Fungal Divers.* **2015**, *74*, 19–51. [\[CrossRef\]](#)
- Rouxel, T.; Balesdent, M.H. The stem canker (blackleg) fungus, *Leptosphaeria maculans*, enters the genomic era. *Mol. Plant Pathol.* **2005**, *6*, 225–241. [\[CrossRef\]](#)
- Roustaeae, A.; Costes, S.; Dechamp-Guillaume, G.; Barrault, G. Phenotypic variability of *Leptosphaeria lindquistii* (anamorph: *Phoma macdonaldii*), a fungal pathogen of sunflower. *Plant Pathol.* **2000**, *49*, 227–234. [\[CrossRef\]](#)
- Sprague, S.J.; Kirkegaard, J.A.; Howlett, B.J.; Graham, J. Effect of root rot and stem canker caused by *Leptosphaeria maculans* on yield of *Brassica napus* and measures for control in the field. *Crop. Pasture Sci.* **2009**, *61*, 50–58. [\[CrossRef\]](#)
- Howlett, B.J.; Idnurm, A.; Pedras, M.S.C. *Leptosphaeria maculans*, the causal agent of blackleg disease of Brassicas. *Fungal Genet. Biol.* **2001**, *33*, 1–14. [\[CrossRef\]](#)
- Descorps, C.; Hebrard, C.; Rakotonindraina, T.; Dechamp-Guillaume, G.; Mestries, E.; Aubertot, J.N. Advances in *Phoma macdonaldii* (*Leptosphaeria lindquistii*) epidemiology. In Proceedings of the 18 International Conference on Sunflower, Barcarce, Argentina, 27 February–1 March 2012; p. 203.
- Claassen, B.J.; Thomas, W.J.; Mallory-Smith, C.; O'Connell, C.M. First report of *Rorippa curvisiliqua* as a host for *Leptosphaeria* spp. (black leg) in North America. *Plant Dis.* **2017**, *101*, 1328. [\[CrossRef\]](#)
- Mendes-Pereira, E.; Balesdent, M.H.; Hortense, B.R.U.N.; Rouxel, T. Molecular phylogeny of the *Leptosphaeria maculans*-*L. biglobosa* species complex. *Mycol. Res.* **2003**, *107*, 1287–1304. [\[CrossRef\]](#)
- Câmara, M.P.S.; Palm, M.E.; van Berkum, P.; O'Neill, N.R. Molecular phylogeny of *Leptosphaeria* and *Phaeosphaeria*. *Mycologia* **2002**, *94*, 630–640. [\[CrossRef\]](#)
- Schoch, C.L.; Seifert, K.A.; Huhndorf, S.; Schindel, D. Nuclear ribosomal internal transcribed spacer (ITS) region as a universal DNA barcode marker for Fungi. *Proc. Natl. Acad. Sci. USA* **2012**, *109*, 6241–6246. [\[CrossRef\]](#)

16. Aveskamp, M.M.; Woudenberg, J.H.; De Gruyter, J.; Turco, E.; Groenewald, J.Z.; Crous, P.W. Development of taxon-specific sequence characterized amplified region (SCAR) markers based on actin sequences and DNA amplification fingerprinting (DAF): A case study in the *Phoma exigua* species complex. *Mol. Plant Pathol.* **2009**, *10*, 403–414. [[CrossRef](#)]
17. Chen, Q.; Jiang, J.R.; Zhang, G.Z.; Cai, L.; Crous, P.W. Resolving the *Phoma* enigma. *Stud. Mycol.* **2015**, *82*, 137–217. [[CrossRef](#)]
18. Armstrong, K.F.; Ball, S.L. DNA Barcodes for biosecurity: Invasive species identification. *Philos. Trans. R. Soc. B* **2005**, *360*, 1813–1823. [[CrossRef](#)]
19. Dilmaghani, A.; Balesdent, M.H.; Didier, J.P.; Wu, C.; Davey, J.; Barbetti, M.J.; Rouxel, T. The *Leptosphaeria maculans*–*Leptosphaeria biglobosa* species complex in the American continent. *Plant Pathol.* **2009**, *58*, 1044–1058. [[CrossRef](#)]
20. Hou, L.W.; Groenewald, J.Z.; Pfenning, L.H.; Yarden, O.; Crous, P.W.; Cai, L. The *phoma*-like dilemma. *Stud. Mycol.* **2020**, *96*, 309–396. [[CrossRef](#)] [[PubMed](#)]
21. Sharma, K.K.; Singh, U.S.; Sharma, P.; Kumar, A.; Sharma, L. Seed treatments for sustainable agriculture—A review. *J. Appl. Nat. Sci.* **2015**, *7*, 521–539. [[CrossRef](#)]
22. Lager, J.; Gerhardson, B. Pathogenicity of clover root pathogens to pea, bean and lucerne. *J. Plant Dis. Protect.* **2002**, *2*, 142–151.
23. Gao, P.; Nan, Z.B.; Christensen, M.J.; Barbetti, M.J.; Duan, T.Y.; Liu, Q.T.; Meng, F.J.; Huang, J.F. Factors influencing rust (*Melampsora apocyni*) intensity on cultivated and wild *Apocynum venetum* in Altay Prefecture, China. *Phytopathology* **2019**, *109*, 593–606. [[CrossRef](#)]
24. White, T.J.; Bruns, T.D.; Lee, S.B.; Taylor, J.W. Amplification and direct sequencing of fungal ribosomal RNA genes for phylogenetics. In *PCR Protocols: A Guide to Methods and Applications*; Academic Press: New York, NY, USA, 1990; pp. 315–322.
25. Liu, Y.J.; Whelen, S.; Hall, B.D. Phylogenetic relationships among ascomycetes: Evidence from an RNA polymerase II subunit. *Mol. Biol. Evol.* **1999**, *16*, 1799–1808. [[CrossRef](#)]
26. Sung, G.H.; Sung, J.M.; Hywel-Jones, N.L.; Spatafora, J.W. A multi-gene phylogeny of Clavicipitaceae (Ascomycota, Fungi): Identification of localized incongruence using a combinational bootstrap approach. *Mol. Phylogenet. Evol.* **2007**, *44*, 1204–1223. [[CrossRef](#)]
27. Vilgalys, R.; Hester, M. Rapid genetic identification and mapping of enzymatically amplified ribosomal DNA from several *Cryptococcus* species. *J. Bacteriol.* **1990**, *172*, 4238–4246. [[CrossRef](#)]
28. Nguyen, L.T.; Schmidt, H.A.; von Haeseler, A.; Minh, B.Q. IQ-TREE: A fast and effective stochastic algorithm for estimating maximum-likelihood phylogenies. *Mol. Biol. Evol.* **2015**, *32*, 268–274. [[CrossRef](#)] [[PubMed](#)]
29. Minh, B.Q.; Nguyen, M.A.; von Haeseler, A. Ultrafast approximation for phylogenetic bootstrap. *Mol. Biol. Evol.* **2013**, *30*, 1188–1195. [[CrossRef](#)]
30. Ronquist, F.; Teslenko, M.; van der Mark, P.; Ayres, D.L.; Darling, A.; Höhna, S.; Larget, B.; Liu, L.; Suchard, M.A.; Huelsenbeck, J.P. MrBayes 3.2: Efficient Bayesian phylogenetic inference and model choice across a large model space. *Syst. Biol.* **2012**, *61*, 539–542. [[CrossRef](#)]
31. Liu, C.L.; Zheng, X.R.; Chen, F.M. Dieback and Leaf Spot in Box Elder (*Acer negundo*) Caused by *Exserohilum rostratum*. *Plant Dis.* **2021**, *105*, 2955–2963. [[CrossRef](#)] [[PubMed](#)]
32. Xue, L.; Zhang, L.; Yang, X.X.; Huang, X.; Zhou, X.; White, J.F.; Liu, Y.; Li, C. Characterization, phylogenetic analyses, and pathogenicity of *Colletotrichum* species on *Morus alba* in Sichuan Province, China. *Plant Dis.* **2019**, *103*, 2624–2633. [[CrossRef](#)] [[PubMed](#)]
33. Zhang, L.Q.; Song, L.L.; Xu, X.M.; Zou, X.H.; Duan, K.; Gao, Q.H. Characterization and fungicide sensitivity of *Colletotrichum* species causing strawberry anthracnose in eastern China. *Plant Dis.* **2020**, *104*, 1960–1968. [[CrossRef](#)] [[PubMed](#)]
34. Chen, T.; Wu, X.; Dai, Y.; Yin, X.; Zhao, Z.; Zhang, Z.; Li, W.; He, L.; Long, Y. Sensitivity testing of natural antifungal agents on *Fusarium fujikuroi* to investigate the potential for sustainable control of kiwifruit leaf spot disease. *J. Fungi* **2022**, *8*, 239. [[CrossRef](#)]
35. Shoemaker, R.A.; Babcock, C.E.; Irwin, J.A.G. *Massarina walkeri* n. sp., the teleomorph of *Acrocalymma medicaginis* from *Medicago sativa* contrasted with *Leptosphaeria pratensis*, *L. weimeri* n. sp., and *L. viridella*. *Can. J. Bot.* **2011**, *69*, 569–573. [[CrossRef](#)]
36. Boerema, G.H.; de Gruyter, J.; Noordeloos, M.E.; Hamers, M.E.C. *Phoma Identification Manual Differentiation of Species and Infra-Specific Taxa in Culture*; CABI Publishing: Wallingford, UK, 2004; p. 417.
37. Lucas, M.T.; Webster, J. Conidial states of British species of *Leptosphaeria*. *Trans. Br. Mycol. Soc.* **1967**, *50*, 85–121.
38. Kövics, G.J.; Irinyi, L.; Rai, M. Overview of *Phoma*-like fungi on important legumes (Papilionaceous Plants). In *Phoma: Diversity, Taxonomy, Bioactivities, and Nanotechnology*; Springer: Cham, Switzerland, 2022; pp. 65–89.
39. Shang, H. Research brief on leaf spot disease in white clover caused by *Stagonospora meliloti*. *Acta Prataculturae Sin.* **1994**, *3*, 81.
40. Irwin, J.A.G.; Mackie, J.M.; Marney, T.S.; Musial, J.M.; Roberts, S. Incidence of *Stagonospora meliloti* and *Acrocalymma medicaginis* in lucerne crowns and roots in eastern Australia, their comparative aggressiveness to lucerne and inheritance of reaction to *S. meliloti* in lucerne. *Australas. Plant Path.* **2004**, *33*, 61–67. [[CrossRef](#)]
41. Musial, J.M.; Mackie, J.M.; Armour, D.J.; Phan, H.T.T.; Ellwood, S.E.; Aitken, K.S.; Irwin, J.A.G. Identification of QTL for resistance and susceptibility to *Stagonospora meliloti* in autotetraploid lucerne. *Theor. Appl. Genet.* **2007**, *114*, 1427–1435. [[CrossRef](#)]
42. Albrecht, H.R. Effect of disease upon survival of white clover, *Trifolium repens* L., in Alabama. *Agron. J.* **1942**, *34*, 725–730. [[CrossRef](#)]
43. Taylor, J.L. A simple, sensitive, and rapid method for detecting seed contaminated with highly virulent *Leptosphaeria maculans*. *Appl. Environ. Microb.* **1993**, *59*, 3681–3685. [[CrossRef](#)]

44. Zhang, X.; White, R.P.; Demir, E.; Jedryczka, M.; Lange, R.M.; Islam, Z.; Li, J.Q.; Huang, A.M.; Hall, G.; Zhou, Z. *Leptosphaeria* spp., phoma stem canker and potential spread of *L. maculans* on oilseed rape crops in China. *Plant Pathol.* **2014**, *63*, 598–612. [[CrossRef](#)]
45. Bonde, M.R.; Nester, S.E.; Berner, D.K. Effects of daily temperature highs on development of *Phakopsora pachyrhizi* on soybean. *Phytopathology* **2012**, *102*, 761–768. [[CrossRef](#)] [[PubMed](#)]
46. Mayorquin, J.S.; Wang, D.H.; Twizeyimana, M.; Eskalen, A. Identification, distribution, and pathogenicity of Diatrypaceae and Botryosphaeriaceae associated with citrus branch canker in the southern California desert. *Plant Dis.* **2016**, *100*, 2402–2413. [[CrossRef](#)] [[PubMed](#)]
47. Morton, V.; Staub, T. A short history of fungicides. *APSnet Features* **2008**, *308*, 1–12. [[CrossRef](#)]
48. Vandenbosch, D.; Braeckmans, K.; Nelis, H.J.; Coenye, T. Fungicidal activity of miconazole against *Candida* spp. biofilms. *J. Antimicrob. Chemoth.* **2010**, *65*, 694–700. [[CrossRef](#)]
49. Zhang, P.; Guan, A.; Xia, X.; Sun, X.; Wei, S.; Yang, J.; Wang, J.; Li, Z.; Lan, J.; Liu, C. Design, synthesis, and structure–activity relationship of new arylpyrazole pyrimidine ether derivatives as fungicides. *J. Agric. Food Chem.* **2019**, *67*, 11893–11900. [[CrossRef](#)] [[PubMed](#)]
50. Teramoto, A.; Meyer, M.C.; Suassuna, N.D.; Cunha, M.G.D. In vitro sensitivity of *Corynespora cassiicola* isolated from soybean to fungicides and field chemical control of target spot. *Summa Phytopathol.* **2017**, *43*, 281–289. [[CrossRef](#)]
51. Camiletti, B.X.; Lichtemberg, P.S.; Paredes, J.A.; Carraro, T.A.; Velascos, J.; Michailides, T.J. Characterization, pathogenicity, and fungicide sensitivity of *Alternaria* isolates associated with preharvest fruit drop in California citrus. *Fungal Biol.* **2022**, *126*, 277–289. [[CrossRef](#)]

Disclaimer/Publisher’s Note: The statements, opinions and data contained in all publications are solely those of the individual author(s) and contributor(s) and not of MDPI and/or the editor(s). MDPI and/or the editor(s) disclaim responsibility for any injury to people or property resulting from any ideas, methods, instructions or products referred to in the content.